Impact of Structural Changes on Multifocal Electroretinography in Patients With Use of Hydroxychloroquine

Enrico Borrelli,[1,2] Marco Battista,[1,2] Maria Lucia Cascavilla,[1] Chiara Viganò,[1,2] Federico Borghesan,[1,2] Nicolò Nicolini,[1,2] Lidia Clemente,[2,3] Riccardo Sacconi,[1,2] Costanza Barresi,[1,2] Alessandro Marchese,[1,2] Elisabetta Miserocchi,[1,2] Giulio Modorati,[1,2] Francesco Bandello,[1,2] and Giuseppe Querques[1,2]

[1]Vita-Salute San Raffaele University Milan, Milan, Italy
[2]IRCCS San Raffaele Scientific Institute, Milan, Italy
[3]Department of Neuroscience, Reproductive Sciences and Dentistry, University of Naples Federico II, Naples, Italy

Correspondence: Giuseppe Querques, Department of Ophthalmology, University Vita-Salute San Raffaele, Via Olgettina 60, Milan, Italy; giuseppe.querques@hotmail.it; querques.giuseppe@unisr.it.

Received: April 17, 2021
Accepted: September 3, 2021
Published: September 28, 2021

Citation: Borrelli E, Battista M, Cascavilla ML, et al. Impact of structural changes on multifocal electroretinography in patients with use of hydroxychloroquine. *Invest Ophthalmol Vis Sci.* 2021;62(12):28. https://doi.org/10.1167/iovs.62.12.28

Purpose. To investigate the relationship between retinal structure and macular function in eyes screened for hydroxychloroquine (HCQ) toxicity.

Methods. Participants referred for hydroxychloroquine retinopathy screening with spectral domain optical coherence tomography (SD-OCT) and multifocal electroretinogram (mfERG) testing were included in the analysis. Amplitude and implicit time of mfERG N1 and P1 responses were included in the analysis. Ring ratios were computed for amplitude values as the ratio of rings 1–3:5 (R1–3:R5). A control group of healthy participants was included for comparison of SD-OCT metrics.

Results. Sixty-three eyes screened for HCQ retinopathy and 30 control eyes were analyzed. The outer nuclear layer (ONL) was significantly thinner in HCQ patients in the foveal ($P = 0.008$), parafoveal ($P < 0.0001$), and perifoveal ($P < 0.0001$) regions. The HCQ cohort was further divided into two subgroups according to the presence of structural clinically detectable retinopathy (i.e., structural damage as detected by multimodal imaging). HCQ eyes without retinopathy had a thinner ONL thickness in the foveal ($P = 0.032$), parafoveal ($P < 0.0001$), and perifoveal ($P < 0.0001$) regions and a thinner inner nuclear layer (INL) in the parafoveal region ($P = 0.045$ versus controls). Structural changes in HCQ patients without retinopathy were significantly associated with macular function as R2:R5 ring ratio of mfERG P1 amplitude was associated with INL ($P = 0.002$) and ONL ($P = 0.044$) thicknesses, and R3:R5 ring ratio of P1 amplitude was associated with ONL thickness ($P = 0.004$).

Conclusions. Our results suggest that structural alterations secondary to HCQ toxicity may occur in the absence of clinically detectable retinopathy, and this may reflect in an impaired macular function.

Keywords: hydroxychloroquine, electroretinogram, image analysis, retina

Hydroxychloroquine (HCQ) is a disease-modifying antirheumatic drug frequently prescribed to treat rheumatic and dermatologic diseases.[1] Although HCQ is known to be a safe and efficacious drug, its long-term use may result in retinal toxicity, which remains a widely recognized side effect.[2] In detail, HCQ retinopathy is characterized by an irreversible photoreceptor and retinal pigment epithelium (RPE) loss with associated retinal dysfunction.[3–6] Automated visual field (VF) and structural optical coherence tomography (OCT) represent the primary screening tests for HCQ retinopathy.[7] Additional tests include multifocal electroretinogram (mfERG) and fundus autofluorescence.[7]

The diagnosis and characterization of HCQ retinopathy is a relevant clinical application of structural OCT. Assuming that OCT provides anatomic information regarding the retinal and RPE layers, this imaging modality may display an early loss of these structures secondary to HCQ toxicity. Based on OCT findings, previous studies[8–11] proposed staging HCQ retinopathy based on the presence and extension of photoreceptor and RPE loss. More recently, Garrity et al.[12] demonstrated that an attenuation of the ellipsoid zone (EZ), rather than a recognizable loss, may precede visual field defects in patients undergoing HCQ therapy, the latter feature suggesting that this may represent the earliest finding of retinal toxicity on OCT images.

The multifocal electroretinogram is an objective technique used to quantify retinal electrical responses reflecting postreceptoral retinal function. Previous evidence suggests that the mfERG test may be employed as part of baseline and/or screening testing in patients under treatment

with HCQ.[7] More important, the mfERG test proved to be capable of detecting early subtle electrophysiologic changes secondary to retinal cells' stress in patients undergoing HCQ therapy, which may be also antecedent to a visible photoreceptor loss detectable on OCT.[13,14] As a consequence, mfERG may be the most sensitive modality to identify early signs of HCQ-associated retinal toxicity, even in the absence of structural clinically detectable retinopathy.[13,14] In addition, mfERG is a valuable tool to identify correlations between anatomic changes and retinal function as it furnishes topographical information on the retinal response across the posterior pole.[15]

What is lacking is information concerning the relationship between the morphologic characteristics detected with structural OCT and retinal function tested with mfERG in participants under treatment with HCQ. Therefore, in this study, we performed a qualitative and quantitative analysis on OCT images from patients screened for HCQ retinopathy to characterize morphologic characteristics correlating with retinal function in these patients. Importantly, a main purpose was to assess associations between morphologic and functional changes in eyes without evidence of detectable retinopathy.

Methods

The San Raffaele Ethics Committee was notified about this retrospective cohort study. The study adhered to the 1964 Declaration of Helsinki and its later amendments. An informed consent waiver was granted to allow retrospective analysis of the previously collected data. In this study, participants 18 years and older who were being treated with HCQ were identified from the medical records of an ophthalmology practice at the San Raffaele Scientific Institute.

To be included in this analysis, patients had to have been imaged during a screening visit for HCQ toxicity with the spectral domain (SD) Heidelberg Spectralis HRA+OCT device (Heidelberg Engineering, Heidelberg, Germany) between January 2017 and January 2021. Each set of SD-OCT scans consisted of 19 B-scans, each of which comprised 24 averaged scans, covering an approximately 5.5 × 4.5-mm area centered on the fovea. A minimum signal strength of 25 was required to the SD-OCT images to be included, as recommended by the manufacturer.[16] Furthermore, patients were required to have a mfERG test (Retimax CSO, Florence, Italy) obtained on the same day. Finally, all patients underwent a complete ophthalmologic examination, which included the measurement of best-corrected visual acuity (BCVA) and dilated fundus examination. The BCVA for each eye was converted to the logMAR, as previously described.[17] Medical history, including details of HCQ dosing, was collected for each patient. Exclusion criteria included (1) presence of any retinal pathology and/or optic nerve disease other than HCQ retinopathy, (2) use of other drugs that are known to be potentially causative of retinal toxicity (e.g., tamoxifen), and (3) refractive error higher than 3 diopters. The analyzed study cohort was divided into two subgroups according to the presence of clinically detectable retinopathy, yielding a group of eyes without retinopathy and a group of eyes with clinically recognizable HCQ retinopathy. HCQ retinopathy was detected based on fundus examination, fundus autofluorescence, and structural SD-OCT, as previously reported.[8–11]

Since age may affect retinal features measured using structural SD-OCT,[18,19] a control group matched for age was also included in the current analysis. All controls had a refractive error of less than 3 diopters and no evidence of retinal disease as evaluated by dilated fundus examination and structural SD-OCT.

OCT Grading

Structural SD-OCT images at the study visit were first reviewed for eligibility by two independent and experienced readers (EB and RS). Successively, the Spectralis built-in software was employed to generate nerve fiber layer (NFL), ganglion cell layer (GCL), inner plexiform layer (IPL), inner nuclear layer (INL), outer plexiform layer (OPL), and outer nuclear layer (ONL) thicknesses, respectively, as previously described.[20] These retinal thicknesses were tested within the circle of the Early Treatment Diabetic Retinopathy Study (ETDRS) grid centered over the fovea. Measurements were automatically averaged across each of the following subfields: the central fovea subfield within the inner 1-mm-diameter circle, the inner circle subfield between the inner and middle 3-mm-diameter circles, and the outer circle subfield between the middle and outer 6-mm-diameter circles. Before computing the thickness values, the graders evaluated all B-scans and manually corrected any segmentation or decentration errors. Cases with segmentation errors that were not reliably correctable were excluded from the analysis.

mfERG

Multifocal ERG (Retimax CSO, Florence, Italy) was recorded for each patient, according to the International Society for Clinical Electrophysiology of Vision (ISCEV) protocol.[21,22] First, pupils were dilated to at least 7 mm with 1% tropicamide. Assuming that retinal adaptation may affect mfERG values, participants were exposed to the same preexposure light, and the examination room's illumination was moderate and the same for all participants. With a 45-in. OLED monitor, an array of 61 hexagons was projected, driven at a frame of 75 Hz, covering the central 40-degree area surrounding the fovea. The black and white hexagons had a luminance of 400 and 1 cd/m^2, respectively. DTL Plus electrodes (Diagnosys LLC, Lowell, MA, USA) were applied on the conjunctiva at the inferior limbus. The ground electrode was attached to the forehead. Before starting the examination, patients were invited to fix a red target on the center of the pattern and required to distinctly perceive this fixation target. Also, the eye's position was observed using a video system. The examination was done monocularly, with a registration time of at least 4 minutes per eye, and repeated in case of eccentric fixation, unstable fixation, or presence of movement artifacts. Signals were processed through a 5- to 100-Hz bandpass filter and amplified through a 30,000 gain. The amplitudes and implicit times of N1 (first negative component) and P1 (first positive component) of the first-order kernel were measured for five regional ring groups (ring 1, R1; ring 2, R2; ring 3, R3; ring 4, R4; and ring 5, R5). N1's amplitude was measured from the baseline to the first negative peak. The amplitude of P1 was measured from the first negative peak to the first positive peak. The implicit times were defined as the time period from the stimulus onset to the peak of N1 and P1 responses. The responses from the central three rings (R1, R2, and R3) were included in the analysis as these rings approximately cover the foveal, parafoveal, and perifoveal regions of the ETDRS grid, respectively.[23,24] The latter choice was made in order to perform correlation analyses between topographically correspondent regions

(R1 and foveal region on SD-OCT, R2 and parafoveal region on SD-OCT, R3 and perifoveal region on SD-OCT). Ring ratios were computed for amplitude values as the ratio of rings 1–3:5.[25]

For each ring, we also collected the response amplitude density (RAD) between the first negative peak N1 and the first positive peak P1 (N1-P1 RAD, expressed in nV/degree^2), as previously reported.[26] The built-in software compares the RAD values against a normal age-matched database to assess whether the participants' RAD values are normal or reduced.

Statistical Analysis

The Statistical Package for Social Sciences (version 23.0; SPSS Inc., Chicago, IL, USA) was employed to perform statistical calculations. Departures from normality distribution were tested with a Shapiro–Wilk's test. Categorial variables were compared by performing a Fisher's exact test. All quantitative variables were presented as mean and standard deviation (SD) in the results.

Continuous variables were compared by conducting a Student's *t*-test for independent variables or an independent-samples Mann–Whitney *U* test or a one-way ANOVA with Tukey's post hoc test. The false discovery rate correction (FDR) was used to control the family-wise type I error rate, and an FDR-adjusted P value <0.05 was determined to be statistically significant.

In regression analyses, only one eye (the right eye in patients with either eye initially included in the analysis) for each HCQ patient was included. A multivariate regression analysis between SD-OCT metrics (dependent variables) and clinical characteristics was performed. Univariate regression analyses of potential associations between structural SD-OCT and functional parameters were performed. Of note, this analysis was performed by investigating the presence of correlations between variables assessing the same macular region (i.e., mfERG ring 1 and SD-OCT foveal region, mfERG ring 2 and SD-OCT parafoveal region, and mfERG ring 3 and SD-OCT perifoveal region, respectively).

Results

Characteristics of Patients Included in the Analysis

Of the 67 participants included in this analysis, 37 patients (63 eyes) were being treated with HCQ, and 30 were healthy controls. All patients and controls were Caucasians. Two of 37 patients had a diagnosis of type 2 diabetes without evidence of diabetic retinopathy. Considering the HCQ group, 11 individual eyes were excluded for unilateral unreliable tests (8 eyes) or concomitant pathologic disorders (3 eyes). Nine (24.3%) patients were taking hydroxychloroquine for rheumatoid arthritis, five (13.5%) were being treated for systemic lupus erythematosus, and the remaining patients were being treated for Sjögren syndrome, mixed connective tissue disease, or other connective tissue disorders. The overall demographic and clinical characteristics of the two groups are shown in Table 1.

Anatomic Metrics

The IPL thickness in the perifoveal region was 28.6 ± 3.7 µm and 30.3 ± 3.3 µm in HCQ patients and controls, respectively ($P = 0.033$) (Table 2, Supplementary Fig. S1).

The ONL thickness significantly differed between HCQ patients and healthy controls in the foveal (85.9 ± 13.8 µm and 94.2 ± 13.8 µm, $P = 0.008$), parafoveal (61.7 ± 10.5 µm and 72.0 ± 9.2 µm, $P < 0.0001$), and perifoveal (52.3 ± 7.3 µm and 58.2 ± 7.4 µm, $P < 0.0001$) regions (Table 2, Supplementary Fig. S1). No other significant changes were detectable between the two groups (Table 2, Supplementary Fig. S1).

The HCQ cohort was further divided into two subgroups according to the presence of structural clinically detectable retinopathy. Forty-six eyes showed absence of HCQ retinopathy, while 17 eyes were characterized by evidence of retinopathy. Clinical severity of HCQ retinopathy based on structural SD-OCT[8,9] was early disease in 14 eyes, moderate in 2 eyes, and advanced in 1 eye, respectively. In this additional analysis, HCQ eyes without retinopathy were characterized by a lower ONL thickness in the foveal (86.0 ± 14.4 µm and 94.2 ± 13.8 µm, $P = 0.032$), parafoveal (62.7 ± 10.1 µm and 72.0 ± 9.2 µm, $P < 0.0001$), and perifoveal (53.3 ± 7.3 µm and 58.2 ± 7.4 µm, $P < 0.0001$) regions, as compared with healthy controls (Table 3). Furthermore, the INL thickness in the parafoveal region was 37.1 ± 3.3 µm and 39.5 ± 3.6 µm in HCQ patients without retinopathy and controls, respectively ($P = 0.045$) (Table 3). Although no significant differences were detected in ONL thickness between patients with and without retinopathy, a scatterplot of ONL values in each disease severity showed a progressive ONL thinning throughout the disease stages (standardized β coefficient = −0.184 and $P = 0.148$ in the foveal region, standardized β coefficient = −0.239 and $P = 0.059$ in the parafoveal region, and standardized ßβ coefficient = −0.385 and $P = 0.002$ in the perifoveal region) (Supplementary Fig. S2).

Table 1. Characteristics of HCQ Patients and Controls

Characteristic	HCQ	HCQ Without Retinopathy	HCQ With Retinopathy	Controls	*P* Value
Eyes enrolled (patients), *n* (%)	63 (37)	46 (27)	17 (10)	30 (30)	—
Age, mean (SD), y	55.8 (14.0)	55.0 (12.9)	57.9 (16.7)	55.8 (17.6)	0.998*
Gender, *n* (%)					
Male	10 (27.0%)	7 (25.9%)	3 (30.0%)	13 (43.3%)	0.200†
Female	27 (73.0%)	20 (74.1%)	7 (70.0%)	17 (56.7%)	
BCVA, mean (SD), logMAR	0.04 (0.06)	0.02 (0.04)	0.05 (0.07)	0.00 (0.00)	<0.0001*
Duration of HCQ therapy, mean (SD), y	8.4 (5.4)	7.6 (5.4)	10.5 (5.3)	—	0.094‡
Cumulative HCQ dose, mean (SD), mg	782.8 (530.1)	704.3 (522.4)	973.4 (538.2)	—	0.115‡

* *t*-test (HCQ vs. controls).
† Fisher's exact test (HCQ vs. controls).
‡ *t*-test (HCQ without retinopathy vs. HCQ with retinopathy).

Table 2. Tested Optical Coherence Tomography Variables in HCQ Patients and Controls

OCT Quantitative Values	Groups, Mean (SD)		*P* Value
	HCQ ($n = 63$)	Controls ($n = 30$)	
Foveal NFL thickness, µm	12.8 (2.6)	12.4 (2.1)	0.439
Foveal GCL thickness, µm	16.5 (7.0)	14.8 (4.1)	0.156
Foveal IPL thickness, µm	21.6 (5.8)	20.7 (3.8)	0.384
Foveal INL thickness, µm	20.3 (6.1)	20.3 (5.4)	0.958
Foveal OPL thickness, µm	27.7 (6.4)	27.6 (6.2)	0.934
Foveal ONL thickness, µm	85.9 (13.8)	94.2 (13.5)	0.008*
Parafoveal NFL thickness, µm	22.8 (2.9)	21.8 (2.5)	0.089
Parafoveal GCL thickness, µm	48.5 (7.4)	49.6 (7.3)	0.503
Parafoveal IPL thickness, µm	40.6 (5.0)	41.6 (4.5)	0.382
Parafoveal INL thickness, µm	38.6 (4.2)	39.5 (3.6)	0.298
Parafoveal OPL thickness, µm	33.9 (4.1)	32.8 (4.3)	0.235
Parafoveal ONL thickness, µm	61.7 (10.5)	72.0 (9.2)	<0.0001*
Perifoveal NFL thickness, µm	36.2 (6.1)	35.3 (6.4)	0.540
Perifoveal GCL thickness, µm	34.8 (5.1)	36.0 (4.9)	0.248
Perifoveal IPL thickness, µm	28.6 (3.7)	30.3 (3.3)	0.033*
Perifoveal INL thickness, µm	32.2 (3.7)	33.1 (2.6)	0.169
Perifoveal OPL thickness, µm	27.9 (2.1)	27.6 (2.3)	0.437
Perifoveal ONL thickness, µm	52.3 (7.3)	58.2 (7.4)	<0.0001*

Values were compared by independent-samples *t*-test.
* Significative *P* value.

Table 3. Tested Optical Coherence Tomography Variables in the Two HCQ Subgroups and in Controls

OCT Quantitative Values	HCQ Without Retinopathy ($n = 46$), Mean (SD)	HCQ With Retinopathy ($n = 17$), Mean (SD)	Controls ($n = 30$), Mean (SD)	*P* Value		
				HCQ Without Retinopathy vs. Controls	HCQ With Retinopathy vs. Controls	HCQ Without Retinopathy vs. HCQ With Retinopathy
Foveal NFL thickness, µm	13.0 (2.8)	12.2 (2.1)	12.4 (2.1)	0.555	0.974	0.521
Foveal GCL thickness, µm	16.8 (7.6)	15.7 (4.9)	14.8 (4.1)	0.380	0.889	0.815
Foveal IPL thickness, µm	21.8 (6.2)	21.1 (4.6)	20.7 (3.8)	0.654	0.978	0.866
Foveal INL thickness, µm	19.4 (5.7)	22.9 (6.2)	20.3 (5.4)	0.784	0.280	0.078
Foveal OPL thickness, µm	27.5 (6.4)	28.1 (6.6)	27.6 (6.2)	1.0	0.965	0.957
Foveal ONL thickness, µm	86.0 (14.4)	85.8 (12.6)	94.2 (13.5)	0.032*	0.045*	0.999
Parafoveal NFL thickness, µm	22.8 (2.7)	22.5 (3.6)	21.8 (2.5)	0.233	0.632	0.916
Parafoveal GCL thickness, µm	48.9 (6.5)	47.3 (9.4)	49.6 (7.3)	0.923	0.572	0.725
Parafoveal IPL thickness, µm	40.9 (4.6)	39.8 (6.0)	41.6 (4.5)	0.852	0.473	0.700
Parafoveal INL thickness, µm	37.1 (3.3)	41.1 (5.4)	39.5 (3.6)	0.045	0.352	0.006*
Parafoveal OPL thickness, µm	33.8 (3.8)	34.2 (4.9)	32.8 (4.3)	0.568	0.477	0.914
Parafoveal ONL thickness, µm	62.7 (10.1)	58.9 (11.1)	72.0 (9.2)	0.0001*	0.0001*	0.373
Perifoveal NFL thickness, µm	36.2 (5.7)	36.0 (7.4)	35.3 (6.4)	0.806	0.928	0.992
Perifoveal GCL thickness, µm	35.3 (5.1)	33.3 (4.9)	36.0 (4.9)	0.805	0.172	0.337
Perifoveal IPL thickness, µm	28.9 (3.9)	27.5 (3.0)	30.3 (3.3)	0.229	0.042*	0.569
Perifoveal INL thickness, µm	32.0 (3.7)	32.7 (3.6)	33.1 (2.6)	0.348	0.910	0.759
Perifoveal OPL thickness, µm	27.7 (2.0)	28.7 (2.3)	27.6 (2.3)	0.961	0.236	0.282
Perifoveal ONL thickness, µm	53.3 (7.3)	49.6 (6.7)	58.2 (7.4)	0.011*	0.0001*	0.168

Values were compared by one-way ANOVA, followed by Tukey's post hoc test.
* Significative *P* value.

In multiple regression analysis, the perifoveal OPL and ONL thicknesses were negatively associated with duration of HCQ therapy ($P = 0.041$ and $P = 0.045$, respectively) (Supplementary Table S1). The perifoveal OPL thickness was associated with age ($P = 0.044$, Supplementary Table S1).

Regression Analysis Between Anatomic and mfERG Metrics

mfERG N1 amplitudes were −0.55 ± 0.30 µV, −0.39 ± 0.22 µV, −0.32 ± 0.22 µV, −0.28 ± 0.22 µV, and −0.22 ± 0.25 µV in the R1 to R5 rings, respectively. mfERG P1 amplitudes were 0.91 ± 0.38 µV, 0.63 ± 0.36 µV, 0.59 ± 0.32 µV, 0.52 ± 0.33 µV, and 0.54 ± 0.37 µV in the R1 to R5 rings, respectively (Fig. 1).

mfERG N1 implicit times were 20.4 ± 8.0 ms, 19.8 ± 7.5 ms, 18.2 ± 7.5 ms, 17.8 ± 7.8 ms, and 17.2 ± 6.5 ms in the R1 to R5 rings, respectively. mfERG P1 implicit times were 38.8 ± 5.5 ms, 37.6 ± 4.6 ms, 36.4 ± 4.1 ms, 34.6 ± 6.8 ms, and 34.0 ± 5.8 ms in the R1 to R5 rings, respectively. Supplementary Table S2 summarizes mfERG results in patients with and without retinopathy.

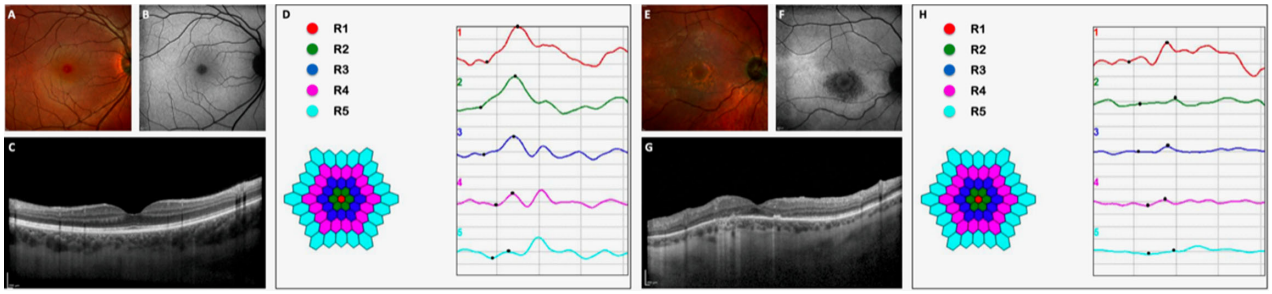

Figure 1. Multimodal imaging and multifocal electroretinogram of two HCQ patients without (**A–D**) and with retinopathy (**E–H**). (**A**) Multicolor image and (**B**) blue-light fundus autofluorescence show a normal appearance of the macula. (**C**) The structural optical coherence tomography B-scan qualitatively shows a normal structure of the macula. (**D**) Amplitudes and latencies of N1 (first negative component) and P1 (first positive component) of the first-order kernel were recorded for five regional ring groups (R1, R2, R3, R4, and R5). P1 amplitude was 1.07 µV, 0.85 µV, 0.77 µV, 0.54 µV, and 0.20 µV in R1, R2, R3, R4, and R5, respectively. N1 amplitude was −0.31 µV, −0.42 µV, −0.34 µV, −0.16 µV, and −0.10 µV in R1, R2, R3, R4, and R5, respectively. (**E**) Multicolor image shows areas of RPE alteration and mottling in the macula. (**F**) Blue-light fundus autofluorescence illustrates a hypoautofluorescent area near the fovea, corresponding to atrophy of the retinal pigment epithelium and outer retina, as confirmed by structural OCT (**G**). (**H**) Multifocal electroretinogram showed a significant reduction in response amplitudes. P1 amplitude was 0.39 µV, 0.09 µV, 0.22 µV, 0.07 µV, and 0.24 µV in R1, R2, R3, R4, and R5, respectively. N1 amplitude was −0.60 µV, −0.22 µV, −0.12 µV, −0.17 µV, and −0.12 µV in R1, R2, R3, R4, and R5, respectively.

In the comparison with the normative database, RAD values were reduced in 10 eyes in ring 1, 13 eyes in ring 2, 14 eyes in ring 3, 14 eyes in ring 4, and 9 eyes in ring 5.

In univariate analysis considering the cohort of HCQ eyes regardless the presence of retinopathy, mfERG P1 amplitude in ring 2 was found to have a significant direct relationship with GLC ($P = 0.047$), IPL ($P = 0.017$), and ONL ($P = 0.046$) thicknesses (Supplementary Table S3). Moreover, mfERG P1 amplitude in ring 3 was statistically associated with IPL thickness by univariate regression analysis ($P = 0.040$) (Supplementary Table S3). mfERG N1 amplitude in ring 1 was found to have significant inverse relationship with NFL thickness ($P = 0.033$) (Supplementary Table S3). Results of univariate linear regressions in the two HCQ groups (with and without retinopathy) are summarized in Supplementary Tables S4 and S5. In patients with retinopathy, significant associations were found between R1N1A and NFL thickness ($P < 0.0001$), R2P1A and ONL thickness ($P = 0.048$), R3N1A and GCL thickness ($P = 0.026$), R3N1A and IPL thickness ($P = 0.032$), R3P1A and GCL thickness ($P = 0.045$), R3P1A and IPL thickness ($P = 0.027$), and R3P1A and OPL thickness ($P = 0.049$) (Supplementary Table S4). In patients without retinopathy, significant associations were found between R2P1A and INL thickness ($P = 0.008$) (Supplementary Table S5).

We also performed univariate analyses with mfERG amplitude values normalized to ring 5 as this approach proved to be advantageous in HCQ eyes without retinopathy.[25,27–29] In this analysis within patients without clinically detectable retinopathy, the R2:R5 ring ratio of mfERG P1 amplitude was statistically associated with INL ($P = 0.002$, Fig. 2) and ONL ($P = 0.044$) thicknesses (Table 4). The R3:R5 ring ratio of mfERG P1 amplitude was found to have a significant direct relationship with ONL thickness ($P = 0.004$) (Table 4, Fig. 2).

Discussion

In this cross-sectional study, we report quantitative data of the macular structure in patients screened for HCQ retinopathy using structural SD-OCT. Overall, we found that retinal layers are significantly affected in HCQ patients. More

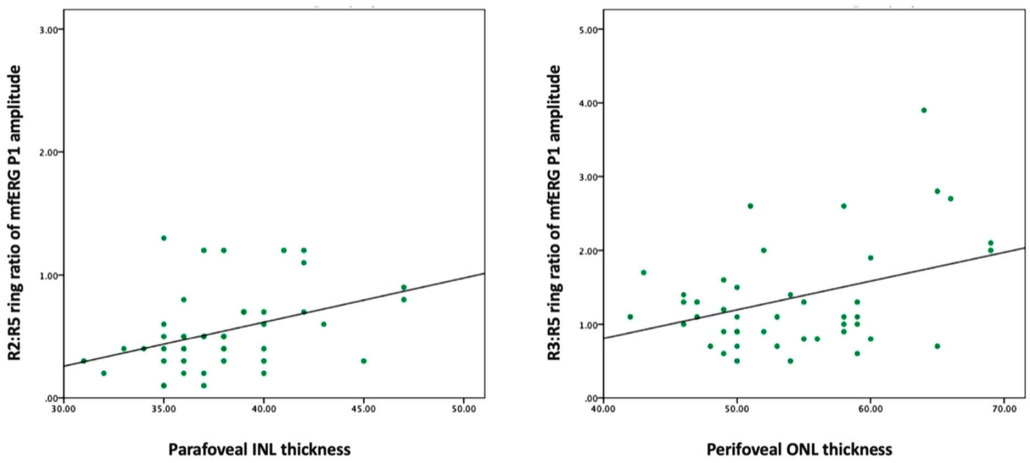

Figure 2. Scatterplots illustrating univariate regression analysis between the mfERG ring ratios (set as dependent variable) and the structural information in HCQ patients without detectable retinopathy. (*Left*) Relationship between the R2:R5 ring ratio of mfERG P1 amplitude and INL thickness ($P = 0.002$). (*Right*) Relationship between the R3:R5 ring ratio of mfERG P1 amplitude and ONL thickness ($P = 0.004$).

Table 4. Univariate Analysis Between OCT Parameters and mfERG Amplitude Ratios in HCQ Patients Without Retinopathy

	NFL Thickness		GCL Thickness		IPL Thickness		INL Thickness		OPL Thickness		ONL Thickness	
Characteristic	Standardized ß Coefficient	*P* Value	Standardized ß Coefficient	*P* Value	Standardized ß Coefficient	*P* Value	Standardized ß Coefficient	*P* Value	Standardized ß Coefficient	*P* Value	Standardized ß Coefficient	*P* Value
R1:R5 N1A	−0.098	0.534	−0.108	0.492	−0.105	0.502	−0.115	0.463	0.268	0.082	0.149	0.340
R1:R5 P1A	0.234	0.132	0.111	0.480	0.205	0.188	0.043	0.784	0.080	0.608	0.070	0.655
R2:R5 N1A	−0.054	0.731	−0.152	0.331	−0.100	0.525	0.088	0.574	0.071	0.653	0.115	0.462
R2:R5 P1A	−0.008	0.961	0.145	0.352	0.187	0.230	0.462	0.002*	0.019	0.906	0.312	0.044*
R3:R5 N1A	0.040	0.800	−0.246	0.111	−0.108	0.491	−0.233	0.132	−0.032	0.840	−0.144	0.356
R3:R5 P1A	−0.085	0.587	−0.053	0.734	−0.086	0.585	−0.105	0.504	0.132	0.399	0.434	0.004*

R1:R5 N1A, ratio between first negative component amplitude values in ring 1 and ring 5; R1:R5 P1A, ratio between first positive component amplitude values in ring 1 and ring 5; R2:R5 N1A, ratio between first negative component amplitude values in ring 2 and ring 5; R2:R5 P1A, ratio between first positive component amplitude values in ring 2 and ring 5; R3:R5 N1A, ratio between first negative component amplitude values in ring 3 and ring 5; R1:R5 P1A, ratio between first positive component amplitude values in ring 3 and ring 5.

* Significative *P* value.

important, we demonstrated that changes in retinal structure are associated with macular function as assessed with multifocal ERG. Therefore, our results suggest that in patients treated with HCQ, there appears to be some pathologic dependence between neuroretinal structures and macular function, even in the absence of apparent structural damage (i.e., HCQ clinically detectable retinopathy).

Several authors have investigated the neuroretinal individual layers' thicknesses in patients screened for HCQ retinopathy. Most of these studies demonstrated inner and outer retinal thinning.[30,31]

Lee et al.[30] examined the ganglion cell complex (i.e., layer combining the IPL and GCL) thickness using structural OCT in 101 patients who ranged in duration of treatment from 2 to 174 months and illustrated a progressive ganglion cell complex (GCC) thinning that weakly correlated with cumulative HCQ dose. Moreover, a GCC thinning was not appreciable in patients without apparent retinopathy, the latter finding suggesting this may not represent an early sign of HCQ toxicity.[30] Conversely, the GCC thickness was significantly reduced in patients with HCQ retinopathy.[30] The GCC thickness in patients screened for HCQ toxicity was also investigated by de Sisternes and colleagues.[32] In the latter study, the authors analyzed structural OCT images from 27 patients screened for HCQ retinal toxicity and without evidence of retinopathy. Patients were divided into two subgroups, according to treatment duration, yielding a group of 12 cases who used the drug less than 5 years and 15 cases with a history of HCQ therapy longer than 15 years. The authors concluded that GCC thickness is not reduced in eyes without evidence of retinopathy and is not associated with increased duration HCQ of use.[32] Similarly, our results showed a significant thinning of the inner retinal layers (i.e., perifoveal IPL) in patients screened for HCQ retinopathy. However, thinning of the inner retina was observed only in patients with evidence of retinopathy. Notably, we did not find associations between treatment duration and/or HCQ cumulative dose and inner retinal layers' thicknesses, as previously suggested.[32] Therefore, HCQ patients seem to be characterized by sparser cells in the perifoveal inner retina, the latter feature eventually secondary to a transneuronal degeneration associated with chronically reduced input to the inner retina secondary to the photoreceptor damage, as previously suggested.[30]

Several authors hypothesized that outer retina thinning may occur in the presence of HCQ toxicity.[33,34] Indeed, it was demonstrated that in eyes with HCQ retinopathy, the outer retina was significantly narrower in eyes with HCQ retinopathy versus control eyes.[33,34] The findings in our study of a reduced ONL thickness in the foveal, parafoveal, and perifoveal regions in the HCQ retinopathy group may indicate a more uniform involvement of the outer retina that may not be otherwise be clinically apparent, as previously suggested.[33] Importantly, this study revealed that perifoveal OPL and ONL thicknesses were negatively associated with duration of HCQ therapy, even after accounting for confounding factors such as age and cumulative dose of HCQ. These results further corroborate previous histopathologic evidence suggesting that chronic exposure to chloroquine may eventually result in degeneration of photoreceptors.[35]

Although outer retinal changes in patients with HCQ retinopathy are well recognized, there has been controversy and even opposing conclusions in the literature on outer retinal modifications occurring in HCQ toxicity without retinopathy.[32,33,36] In our study, we further divided our HCQ cohort into two subgroups according to the presence of retinopathy. Interestingly, in this additional analysis, the reduction in ONL thickness was still significant also in the group without clinically detectable retinopathy. Therefore, our study seems to support the hypothesis that ONL thinning occurs early in HCQ toxicity. A possible limitation to this analysis is that segmentation failure may occur when imaging HCQ patients, resulting in erroneous measurements of the ONL thickness.[32] However, we manually corrected segmentation errors and excluded cases with persistent artifacts from our analysis. Furthermore, cases without retinopathy are not prone to such artifacts as they have a normal retinal architecture for definition. Finally, in contrast to previous studies[31,32] that failed to demonstrate a ONL thinning in HCQ patients without retinopathy, we have a larger cohort (46 eyes in our study versus 16 eyes in the study by Pasadhika et al.[31]) and the presence of an age-matched control group (i.e., in contrast with the study by de Sisternes et al.[32]).

We found that the INL thickness is significantly reduced in HCQ patients without retinopathy. The INL consists of the cell bodies of different cells, including bipolar cells. This is in agreement with previous histopathologic evidence showing that cytoplasmic inclusion bodies and cell loss are prominent in the INL of patients chronically exposed to HCQ.[37] While INL thinning was present in eyes without clinically detectable retinopathy, this difference was not detected in eyes with retinopathy. A possible explanation for the lack of INL thinning in eyes with HCQ retinopathy is mechanical tension to the INL caused by the prominent loss of photoreceptors leading to secondary INL stretching.

We add to the literature by reporting the associations between retinal individual layers' thicknesses and macular

function in HCQ patients. In order to measure macular function, we employed mfERG, which detects functional electrophysiologic changes in bipolar cells, photoreceptors, and, to some extent, inner retinal cells.[38] Multifocal ERG has been historically considered a sensitive technique for the detection of retinal abnormalities in patients screened for HCQ toxicity.[25,27] Importantly, detectable electrophysiologic alterations may precede the visible morphologic changes of tissue destruction detected by structural OCT.[25,27] Therefore, it has been suggested that mfERG test results might represent a better indication of HCQ-related cellular toxicity. Considering the whole cohort of HCQ patients, we found that P1 mfERG amplitude was associated with IPL thickness. Since the P1 wave is known to be influenced by the inner retina,[38] we may speculate that a reduction in inner retinal cells in HCQ patients may affect the postphotoreceptor function. We also found a significant association between P1 amplitude and INL thickness, which was significantly reduced in our study cohort. This result further advises a reduction in bipolar cells in these patients. Furthermore, our results showed that P1 mfERG amplitude was also associated with ONL thickness. As a consequence, our findings would appear to advise that the HCQ-related outer retinal thinning may impair macular function in these patients. Interestingly, we found that these associations were mainly limited to the R2 and R3 rings. This is consistent with previous studies showing that ring 2 and ring 3 P1 amplitudes represent the strongest indicators of disease.[25,27,28]

As explained above, we further split our HCQ cohort into two subgroups according to the presence of retinopathy. Previous important studies already demonstrated that HCQ patients without retinopathy are notable for decreased mfERG metrics.[25,27–29] Of note, these studies showed that normalization to ring 5 of inner rings' values may increase the sensitivity of mfERG to detect subtle function abnormalities and reduce reliance on age correction.[25,27–29] In detail, the R2:R5 ring ratio was displayed to be the most sensitive to detect function abnormalities in HCQ patients without retinopathy.[29] Therefore, we performed an additional analysis to characterize associations between retinal thicknesses and macular functional expressed as ratios to ring 5 in HCQ patients without clinically detectable retinopathy. One of the most notable observations from our study was that R2:R5 and R3:R5 P1 amplitude ratios were significantly associated with INL and ONL thicknesses. Therefore, our findings suggest that photoreceptor and postphotoreceptor alterations secondary to HCQ toxicity may occur in the absence of clinically detectable retinopathy, resulting in an impaired macular function.

Our study has some limitations. First, we did not enroll healthy participants for macular function comparisons. However, this study aimed to assess the presence of subtle anatomic changes in eyes without clinically detectable HCQ retinopathy and to assess associations between these structural alterations and macular function, since other studies have already investigated mfERG changes in patients screened for HCQ toxicity.[25,27,28] In addition, this study was not large enough to account for confounding factors such as age, diabetes, or smoking, which are known to affect electroretinogram values.[39–41] Moreover, shifts in fixation may represent a limitation in assessing associations between pathologic features and functional changes in the central macular region. However, the fixation monitoring system employed during mfERG recordings identified the occurrence of any contamination by blinks or eye movements. Finally, our analysis did not account for presence of an attenuation of the EZ that was demonstrated to potentially precede a photoreceptor defect in patients undergoing HCQ therapy.[12] However, only a small subset of our study cohort (five eyes from three patients) was characterized by this SD-OCT feature. Therefore, we did not have sufficient power to find statistical significance considering these eyes as an additional subgroup.

In summary, we observed that patients screened for HCQ toxicity are characterized by a significant thinning of the inner and outer retina. More important, eyes without evidence of clinically detectable retinopathy are characterized by a significant thinning of the INL and ONL, suggesting that HCQ toxicity may result in an early retinal cell loss. In our morphofunctional analysis, retinal thinning appeared to correlate with macular function by multifocal ERG in HCQ patients without retinopathy. Therefore, our results suggest that structural alterations secondary to HCQ toxicity may occur in the absence of clinically detectable retinopathy, and this may reflect in an impairment of the macular function. Future studies with extended longitudinal follow-up of this cohort may provide additional substantive information. Last, assuming that mfERG testing is not widely available in a clinical setting, structural OCT measures, if replicated in future studies, may prove to be useful biomarkers for screening retinal HCQ toxicity.

Acknowledgments

Disclosure: **E. Borrelli,** None; **M. Battista,** None; **M.L. Cascavilla,** None; **C. Viganò,** None; **F. Borghesan,** None; **N. Nicolini,** None; **L. Clemente,** None; **R. Sacconi,** None; **C. Barresi,** None; **A. Marchese,** None; **E. Miserocchi,** None; **G. Modorati,** None; **F. Bandello,** Alcon (C), Alimera Sciences (C), Allergan Inc (C), Farmila-Thea (C), Bayer Shering-Pharma (C), Bausch and Lomb (C), Genentech (C), Hoffmann-La-Roche (C), Novagali Pharma (C), Novartis (C), Sanofi-Aventis (C), Thrombogenics (C), Zeiss (C); **G. Querques,** Alimera Sciences (C), Allergan Inc (C), Amgen (C), Bayer Shering-Pharma (C), Heidelberg (C), KBH (C), LEH Pharma (C), Lumithera (C), Novartis (C), Sandoz (C), Sifi (C), Sooft-Fidea (C), Zeiss (C)

References

1. Kumar P, Banik S. Pharmacotherapy options in rheumatoid arthritis. *Clin Med Insights Arthritis Musculoskelet Disord*. 2013;6:35–43.
2. Marmor MF, Kellner U, Lai TYY, Lyons JS, Mieler WF. Revised recommendations on screening for chloroquine and hydroxychloroquine retinopathy. *Ophthalmology*. 2011;118(2):415–422.
3. Marmor MF, Hu J. Effect of disease stage on progression of hydroxychloroquine retinopathy. *JAMA Ophthalmol*. 2014;132(9):1105–1112.
4. Marmor MF, Melles RB. Disparity between visual fields and optical coherence tomography in hydroxychloroquine retinopathy. *Ophthalmology*. 2014;121(6):1257–1262.
5. Mititelu M, Wong BJ, Brenner M, Bryar PJ, Jampol LM, Fawzi AA. Progression of hydroxychloroquine toxic effects after drug therapy cessation: New evidence from multimodal imaging. *JAMA Ophthalmol*. 2013;131(9):1187–1197.
6. Lee DH, Melles RB, Joe SG, et al. Pericentral hydroxychloroquine retinopathy in Korean patients. *Ophthalmology*. 2015;122(6):1252–1256.
7. Marmor MF, Kellner U, Lai TYY, Melles RB, Mieler WF, Lum F. Recommendations on screening for chloroquine and

hydroxychloroquine retinopathy (2016 revision). *Ophthalmology*. 2016;123(6):1386–1394.
8. Melles RB, Marmor MF. Pericentral retinopathy and racial differences in hydroxychloroquine toxicity. *Ophthalmology*. 2015;122(1):110–116.
9. Kim KE, Ahn SJ, Woo SJ, et al. Use of OCT retinal thickness deviation map for hydroxychloroquine retinopathy screening. *Ophthalmology*. 2021;128(1):110–119.
10. Allahdina AM, Chen KG, Alvarez JA, Wong WT, Chew EY, Cukras CA. Longitudinal changes in eyes with hydroxychloroquine retinal toxicity. *Retina*. 2019;39(3):473–484.
11. Lally DR, Heier JS, Baumal C, et al. Expanded spectral domain-OCT findings in the early detection of hydroxychloroquine retinopathy and changes following drug cessation. *Int J Retin Vitr*. 2016;2(1):18.
12. Garrity ST, Jung JY, Zambrowski O, et al. Early hydroxychloroquine retinopathy: optical coherence tomography abnormalities preceding Humphrey visual field defects. *Br J Ophthalmol*. 2019;103(11):1600–1604.
13. Lai TYY, Ngai JWS, Chan WM, Lam DSC. Visual field and multifocal electroretinography and their correlations in patients on hydroxychloroquine therapy. *Doc Ophthalmol*. 2006;112(3):177–187.
14. Lyons JS, Severns ML. Detection of early hydroxychloroquine retinal toxicity enhanced by ring ratio analysis of multifocal electroretinography. *Am J Ophthalmol*. 2007;143(5):801–809.
15. Borrelli E, Mastropasqua R, Senatore A, et al. Impact of choriocapillaris flow on multifocal electroretinography in intermediate age-related macular degeneration eyes. *Invest Ophthalmol Vis Sci*. 2018;59(4):AMD25–AMD30.
16. Huang Y, Gangaputra S, Lee KE, et al. Signal quality assessment of retinal optical coherence tomography images. *Invest Ophthalmol Vis Sci*. 2012;53(4):2133–2141.
17. Holladay JT. Proper method for calculating average visual acuity. *J Refract Surg*. 2017;13(4):388–391.
18. Kashani AH, Zimmer-Galler IE, Shah SM, et al. Retinal thickness analysis by race, gender, and age using Stratus OCT. *Am J Ophthalmol*. 2010;149(3):496–502.e1.
19. Alamouti B, Funk J. Retinal thickness decreases with age: an OCT study. *Br J Ophthalmol*. 2003;87(7):899–901.
20. Li ST, Wang XN, Du XH, Wu Q. Comparison of spectral-domain optical coherence tomography for intraretinal layers thickness measurements between healthy and diabetic eyes among Chinese adults. *PLoS One*. 2017;12(5):e0177515.
21. Hood DC, Bach M, Brigell M, et al. ISCEV standard for clinical multifocal electroretinography (mfERG) (2011 edition). *Doc Ophthalmol*. 2012;124(1):1–13.
22. Hoffmann MB, Bach M, Kondo M, et al. ISCEV standard for clinical multifocal electroretinography (mfERG) (2021 update). *Doc Ophthalmol*. 2021;142(1):5–16.
23. Khojasteh H, Riazi-Esfahani H, Khalili Pour E, et al. Multifocal electroretinogram in diabetic macular edema and its correlation with different optical coherence tomography features. *Int Ophthalmol*. 2020;40(3):571–581.
24. Vámos R, Tátrai E, Németh J, Holder GE, DeBuc DC, Somfai GM. The structure and function of the macula in patients with advanced retinitis pigmentosa. *Invest Ophthalmol Vis Sci*. 2011;52(11):8425–8432.
25. Tsang AC, Ahmadi S, Hamilton J, et al. The diagnostic utility of multifocal electroretinography in detecting chloroquine and hydroxychloroquine retinal toxicity. *Am J Ophthalmol*. 2019;206:132–139.
26. Cascavilla ML, Parisi V, Triolo G, et al. Retinal dysfunction characterizes subtypes of dominant optic atrophy. *Acta Ophthalmol*. 2017;96(2):e156–e163.
27. Tsang AC, Ahmadi Pirshahid S, Virgili G, Gottlieb CC, Hamilton J, Coupland SG. Hydroxychloroquine and chloroquine retinopathy: a systematic review evaluating the multifocal electroretinogram as a screening test. *Ophthalmology*. 2015;122(6):1239–1251.e4.
28. Adam MK, Covert DJ, Stepien KE, Han DP. Quantitative assessment of the 103-hexagon multifocal electroretinogram in detection of hydroxychloroquine retinal toxicity. *Br J Ophthalmol*. 2012;96(5):723–729.
29. Lai TYY, Chan W-M, Li H, Lai RYK, Lam DSC. Multifocal electroretinographic changes in patients receiving hydroxychloroquine therapy. *Am J Ophthalmol*. 2005;140(5):794–807.
30. Lee MG, Kim SJ, Ham D Il, et al. Macular retinal ganglion cell–inner plexiform layer thickness in patients on hydroxychloroquine therapy. *Invest Ophthalmol Vis Sci*. 2015;56(1):396–402.
31. Pasadhika S, Fishman GA, Choi D, Shahidi M. Selective thinning of the perifoveal inner retina as an early sign of hydroxychloroquine retinal toxicity. *Eye*. 2010;24(5):756–763.
32. de Sisternes L, Hu J, Rubin DL, Marmor MF. Analysis of inner and outer retinal thickness in patients using hydroxychloroquine prior to development of retinopathy. *JAMA Ophthalmol*. 2016;134(5):511–519.
33. Modi YS, Au A, Parikh VS, Ehlers JP, Schachat AP, Singh RP. Volumetric single-layer inner retinal analysis in patients with hydroxychloroquine toxicity. *Retina*. 2016;36(10):1941–1950.
34. Ugwuegbu O, Uchida A, Singh RP, et al. Quantitative assessment of outer retinal layers and ellipsoid zone mapping in hydroxychloroquine retinopathy. *Br J Ophthalmol*. 2019;103(1):3–7.
35. Rosenthal AR, Kolb H, Bergsma D, Huxsoll D, Hopkins JL. Chloroquine retinopathy in the rhesus monkey. *Invest Ophthalmol Vis Sci*. 1978;17(12):1158–1175.
36. Uslu H, Gurler B, Yildirim A, et al. Effect of hydroxychloroquine on the retinal layers: a quantitative evaluation with spectral-domain optical coherence tomography. *J Ophthalmol*. 2016;2016:8643174.
37. Ramsey MS, Fine BS. Chloroquine toxicity in the human eye histopathologic observations by electron microscopy. *Am J Ophthalmol*. 1972;73(2):229–235.
38. Hood DC, Frishman LJ, Saszik S, Viswanathan S. Retinal origins of the primate multifocal ERG: implications for the human response. *Invest Ophthalmol Vis Sci*. 2002;43(5):1673–1685.
39. Celesia GG, Kaufman D, Cone S. Effects of age and sex on pattern electroretinograms and visual evoked potentials. *Electroencephalogr Clin Neurophysiol*. 1987;68(3):161–171.
40. Bearse MA, Adams AJ, Han Y, et al. A multifocal electroretinogram model predicting the development of diabetic retinopathy. *Prog Retin Eye Res*. 2006;25(5):425–448.
41. Gundogan FC, Erdurman C, Durukan AH, Sobaci G, Bayraktar MZ. Acute effects of cigarette smoking on multifocal electroretinogram. *Clin Experiment Ophthalmol*. 2007;35(1):32–37.

Investigative Ophthalmology & Visual Science